Reactions of Hydrated Electrons $(H_2O)_n^-$ with Carbon Dioxide and Molecular Oxygen: Hydration of the CO_2^- and O_2^- Ions

O. Petru Balaj, Chi-Kit Siu, Iulia Balteanu, Martin K. Beyer,* and Vladimir E. Bondybey*[a]

Abstract: The gas-phase reactions of hydrated electrons with carbon dioxide and molecular oxygen were studied by Fourier transform ion cyclotron resonance (FT-ICR) mass spectrometry. Both CO_2 and O_2 react efficiently with $(H_2O)_n^-$ because they possess low-lying empty π^* orbitals. The molecular CO_2^- and O_2^- anions are concurrently solvated and stabilized by the water ligands to form $CO_2^-(H_2O)_n$ and $O_2^-(H_2O)_n$. Core exchange reactions are also observed, in which $CO_2^-(H_2O)_n$ is transformed into $O_2^-(H_2O)_n$ upon collision with O_2. This is in agreement with the prediction based on density functional theory calculations that $O_2^-(H_2O)_n$ clusters are thermodynamically favored with respect to $CO_2^-(H_2O)_n$. Electron detachment from the product species is only observed for $CO_2^-(H_2O)_2$, in agreement with the calculated electron affinities and solvation energies.

Keywords: gas-phase reactions · hydrated electrons · nanodroplets · radical ions · solvation

Introduction

Most chemical reactions involve a transfer or redistribution of electrons between the reacting species, and free electrons themselves can be considered to be the simplest chemical reactants. Indeed, the reactions of electrons in bulk solutions have been studied quite extensively, for instance in experiments using pulsed radiolysis techniques,[1] and Marcus pioneered the theory of electron-transfer reactions in solution.[2] We have recently pointed out that reactivity studies of solvated electrons in finite clusters, rather than in bulk solutions, could provide very useful complementary information.[3] This approach has the advantages that the elemental compositions of clusters can be unambiguously established based on their exact masses, and that side reactions that limit the lifetime of the hydrated electrons are absent.

All the species involved in the current work, that is, molecular oxygen, water, and carbon dioxide, are important components of the atmosphere. Moreover, electrons are extremely ubiquitous, being formed by radioactive processes, cosmic and vacuum UV radiation, as well as by electric discharges and lightning. In view of the abundance and frequent occurrence of these species, and their importance in relation to atmospheric chemistry, the reactions of aqueous electrons with oxygen and carbon dioxide, and the properties and chemistry of the solvated anions investigated here, may be of more than just academic interest.

The CO_2^- molecular anion, also known as the formate radical, has been repeatedly observed in rare gas matrices and characterized by infrared spectroscopy.[4–9] Free CO_2^- has been generated in a crossed-beam experiment through the collision of alkali metal atoms with CO_2,[10] from which its adiabatic electron affinity was established as $-58 \pm 19\ kJ\,mol^{-1}$, while its vertical electron affinity was determined from electron-scattering measurements as $-350\ kJ\,mol^{-1}$.[11] Calculations by Yoshioka and Jordan confirmed the charge-transfer nature of alkali metal–CO_2 complexes.[12,13] The idea that solvation can stabilize the CO_2^- anion was developed in relation to $(CO_2)_n^-$ clusters.[14–16] Klots found that even one water molecule is sufficient to prevent autodetachment of an electron from $CO_2^-(H_2O)$.[17] Recently, photoelectron spectroscopic studies[18] and ab initio calculations[19] by Nagata, Iwata, and co-workers confirmed and quantified these early observations. Similar results on the stabilization of COS^- by a single water molecule have recently been reported by Sanov and co-workers.[20]

[a] O. P. Balaj, Dr. C.-K. Siu, I. Balteanu, Prov.-Doz. Dr. M. K. Beyer, Prof. Dr. V. E. Bondybey
Institut für Physikalische und Theoretische Chemie
Technische Universität München
Lichtenbergstrasse 4, 85747 Garching (Germany)
Fax: (+49) 89-289-13416
E-mail: beyer@ch.tum.de
bondybey@ch.tum.de

Supporting information for this article is available on the WWW under http://www.chemeurj.org/ or from the author: optimized geometries in Cartesian coordinates, harmonic vibrational frequencies and their IR intensities, and thermochemical data for $CO_2(H_2O)_n$, $CO_2^-(H_2O)_n$, $O_2(H_2O)_n$, $O_2^-(H_2O)_n$, and $(H_2O)_n$ for $n = 1$–5 estimated by calculations at the B3LYP/6-311++G(3df,3pd) level of theory.

DOI: 10.1002/chem.200400416

The superoxide radical, O_2^-, is ubiquitous in radiation chemistry, and plays an important role in biological radiation damage.[21] CO_2^- can serve as an intermediate in its formation.[22] In contrast to CO_2, the electron affinity of O_2 is positive, and no solvent is needed to stabilize the radical anion. Recent infrared spectroscopic studies by Johnson and co-workers indicate that the first solvation shell of $O_2^-(H_2O)_n$ is completed at $n = 4$.[23,24]

Hydrated electrons in the gas phase, $(H_2O)_n^-$, were first reported by Haberland and co-workers,[25–27] and extensively characterized spectroscopically, among others by Bowen and co-workers.[28–30] A series of experiments by the groups of Johnson and Viggiano[31,32] in molecular beam and flow reactor set-ups has revealed an interesting variety in their behavior towards different gaseous reactants. As typical electron scavengers, diatomic O_2, as well as the usually extremely stable and unreactive CO_2 molecules, are "dissolved" in the $(H_2O)_n^-$ with high efficiency.

We have previously reported that a laser vaporization cluster source is an effective source of solvated electrons.[33] This allowed us to investigate in some detail the stability of the solvated electrons, and the competition between their fragmentation and electron detachment induced by ambient black-body infrared radiation. In the present work, we focus our investigation on $O_2^-(H_2O)_n$ and $CO_2^-(H_2O)_n$. The experimental study of the formation and stability of these hydrated anions is complemented by quantum-chemical computations.

Results and Discussion

Reactions of $(H_2O)_n^-$ clusters with carbon dioxide: A typical initial mass spectrum of the hydrated electron clusters produced in our source at a nominal time $t = 0$, that is, immediately after the ion accumulation, is shown in Figure 1 a. As noted above, the distribution of the $(H_2O)_n^-$ clusters generated is somewhat dependent on the source setting, that is, the laser power and its focusing, the pressure of the carrier gas, the pressure of the entrained water vapor, and in particular on the relative timing of the laser pulse and the opening of the valve controlling the gas flow. Even though the exact size range, which in this particular experiment extends between $n = 27$ and $n = 62$, may differ slightly from experiment to experiment, some features of the distribution appear to be well reproducible. Examples are the relatively pronounced maximum of the $n = 50$ cluster, which is almost a factor of two more intense than the $n = 51$ and $n = 49$ peaks, and the even-odd intensity alternation exhibited by the peaks just above $n = 50$.

Even in the nominally $t = 0$ spectrum, some products of the reaction with carbon dioxide are already present. As explained in the Experimental Section, the $(H_2O)_n^-$ clusters produced in the source are usually accumulated over twenty pulses, that is, over nearly 2 s at the 10 Hz laser repetition rate. Since a constant pressure of 7.7×10^{-9} mbar of CO_2 is maintained in the cell, the reaction takes place within this accumulation period. Since the laser has to warm up in the first few shots and some previously trapped ions are lost again in the accumulation cycle, the nominal time $t = 0$ corresponds to about 0.5 s reaction time.

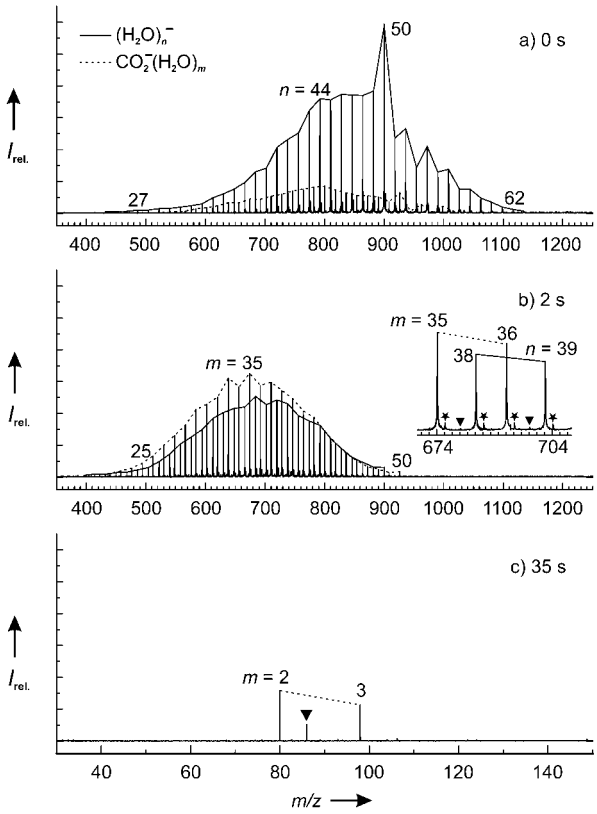

Figure 1. Mass spectra of the reaction of $(H_2O)_n^-$ with CO_2. a) At 0 s, some clusters have already reacted during the accumulation of the hydrated electrons in the ICR cell, and the product species $CO_2^-(H_2O)_m$ are present to some extent. b) After 2 s, more than 50% of the initial $(H_2O)_n^-$ has been converted into products. In parallel, black-body radiation and collision-induced dissociation occurs, and the clusters shrink by loss of single water molecules. For $n<30$, electron loss from $(H_2O)_n^-$ also occurs, but since only few $(H_2O)_n^-$ reach this size region before conversion into $CO_2^-(H_2O)_m$, this reaction is negligible. Only one molecule of CO_2 enters the cluster, and the fragmentation proceeds until the cluster $CO_2^-(H_2O)_2$ is reached, as seen in c) 35 s. These species slowly disappear from the mass spectrum due to electron detachment. In the inset, the peaks marked * are due to the natural abundance of ^{18}O in the water molecules. $O_2^-(H_2O)_p$ impurity peaks, marked ▼, are also present after long reaction delays.

The reaction involves the uptake of one and only one carbon dioxide molecule by the clusters, resulting in $CO_2^-(H_2O)_m$. A careful examination of the spectrum after 2 s (Figure 1 b) reveals that the product clusters have very similar, maybe slightly lower masses than the reactant species. Since the mass of CO_2 of 44 amu corresponds to 2.44 water molecules, this indicates that two to three water molecules are lost upon uptake of the CO_2 molecule by the cluster [Eq. (1)].

$$(H_2O)_n^- + CO_2 \rightarrow CO_2^-(H_2O)_{n-x} + x\,H_2O,\ x = 2-3 \quad (1)$$

An interesting detail concerning the intensity alternation above the intensity maximum is that it is considerably more

pronounced for the products of reaction according to Equation (1) than for the reactant clusters. While the peaks for the odd-numbered solvated electrons in the range $n = 51$–55 are, on average, about 5–15% weaker than those for the neighboring even-numbered clusters, the intensity ratios are much larger for the products, with the odd-numbered clusters being favored by a factor of closer to three or four. Probably, a combination of kinetic and thermochemical effects is responsible for the observation of pronounced "magic numbers" for $CO_2^-(H_2O)_m$, $45 < m < 55$.

Comparison of the integrated intensities of the peaks due to hydrated electrons with those of the carbon dioxide containing $CO_2^-(H_2O)_n$ products (Figure 1b) indicates that within 2 s more than half of the initially present clusters have reacted. This observation, combined with the known CO_2 pressure and the collision rates calculated from ADO theory,[34–36] leads to the conclusion that the reaction efficiency reaches almost 300%. This is not unreasonable, since the collision rate is calculated with reference to a point-charge model, while the reactant cluster has considerable size, and its collision cross-section is therefore larger than that of a point charge.

After the initial exchange, only a gradual fragmentation, due mainly to cluster heating by the room temperature black-body background radiation, takes place, with the water ligands being lost one by one. The final stage of the reaction and of this cluster fragmentation process is illustrated in Figure 1c, which shows the mass spectrum after a reaction time of 35 s. At this point, only weak peaks due to the last two, smallest carbon dioxide containing clusters, $n = 2$ and $n = 3$, remain. Also visible in the spectrum are the fragmentation products of impurity clusters containing molecular oxygen, $O_2^-(H_2O)_3$. No $CO_2^-(H_2O)$ cluster is detected, and after a few additional seconds all the signals due to the CO_2-containing clusters vanish. This is due to electron detachment, with neither the electron itself, nor the remaining, weakly bound neutral cluster, being directly observable in the FT-ICR instrument.

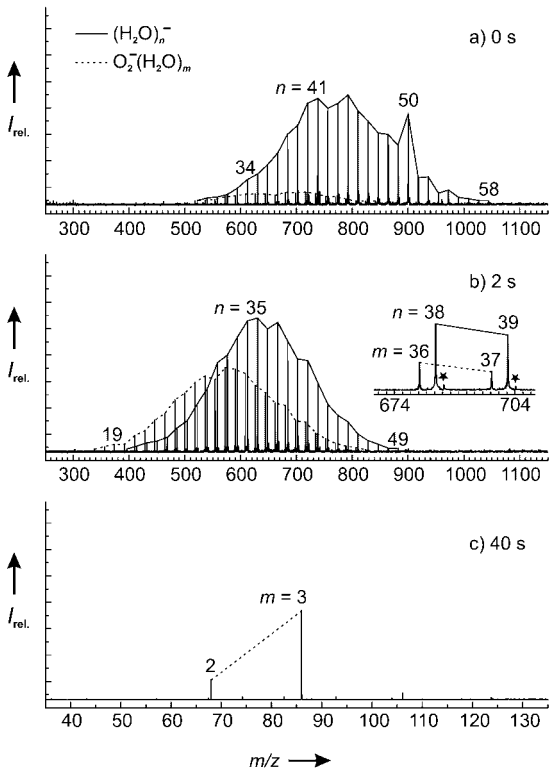

Figure 2. Mass spectra of the reaction of $(H_2O)_n^-$ with O_2. a) At 0 s, some clusters have already reacted during the accumulation of the hydrated electrons in the ICR cell, and the product species $O_2^-(H_2O)_m$ are present to some extent. b) After 2 s, only about 30% of the initial $(H_2O)_n^-$ has been converted into products. In parallel, black-body radiation and collision-induced dissociation occurs, and the clusters shrink by loss of single water molecules. For $n < 30$, electron loss from $(H_2O)_n^-$ also occurs, but since only few $(H_2O)_n^-$ reach this size region before conversion into $O_2^-(H_2O)_m$, this reaction is negligible. Only one molecule of O_2 enters the cluster, and the fragmentation proceeds until the cluster $O_2^-(H_2O)_2$ is reached, as seen in c) 40 s. These species are stable with respect to further fragmentation as well as electron detachment. In the inset, the peaks marked * are due to the natural abundance of ^{18}O in the water molecules.

Reactions of $(H_2O)_n^-$ clusters with O_2: The reactions with molecular oxygen are similar to those with carbon dioxide, in that one and only one O_2 molecule is taken up by each cluster. For the products, the entire distribution seems to be shifted to smaller values of n. After a reaction time of 2 s (Figure 2b), the $(H_2O)_n^-$ distribution has its maximum at around $n = 35$, while the most intense product cluster peak is at $n = 30$, with the shift suggesting that in the case of oxygen, the reaction proceeds according to Equation (2).

$$(H_2O)_n^- + O_2 \rightarrow O_2^-(H_2O)_{n-x} + x\,H_2O,\ x \approx 5-6 \qquad (2)$$

In other words, the dissolution of the O_2 molecule in the cluster is accompanied by the evaporation of several water ligands. This is consistent with the considerably higher exothermicity of the reaction with molecular oxygen. After 2 s (Figure 2b), only 30–40% of the hydrated electrons are converted into products, in spite of the higher O_2 pressure of 1.86×10^{-8} mbar compared to the CO_2 pressure. This yields an ADO collision efficiency of 100%, about one-third of the value for CO_2. The relative values are in agreement with earlier flow-tube results,[32] while the absolute values deviate by a factor of three. However, the different reaction gas temperatures, 100 K in the flow tube compared to 300 K in the present study, may very well explain this discrepancy. Also, the number of water molecules lost is in good agreement with the flow-tube results.

As in the case of carbon dioxide, after the first step, no further O_2 molecules are taken up by the clusters, and again only their gradual fragmentation is observed, with the distribution shifting towards smaller cluster sizes. After some 15 s, almost every cluster has dissolved one O_2 molecule, with the unreacted solvated electron clusters being barely observable. The size distribution of the $O_2^-(H_2O)_n$ products ranges from about $n = 4$ to $n = 12$. The fragmentation continues further but with decreasing rate, so that after some 40 s of reaction time the $n = 3$ cluster is dominant. This loses an additional ligand only very reluctantly to form the $O_2^-(H_2O)_2$ final product (Figure 2c). Unlike in the case of CO_2, however, even after 60 s, which is the longest time

studied, the signals do not disappear, but the $n = 2$ and 3 species remain with comparable intensities.

Ionic core exchange reactions: To learn more about the relative stabilities of $CO_2^-(H_2O)_n$ and $O_2^-(H_2O)_n$, and to ascertain whether the formation of O_2^- from CO_2^- can proceed directly in solution, in a third experiment we studied the exchange of the ionic core. CO_2 was introduced into the UHV at a relatively high partial pressure of 1.3×10^{-7} mbar, together with O_2 at a partial pressure of 5.7×10^{-8} mbar. After 0.5 s (Figure 3a), the $(H_2O)_n^-$ distribution had been completely lost, and $CO_2^-(H_2O)_n$ predominated in the spectrum. After 3 s (Figure 3b), $O_2^-(H_2O)_m$ had become the dominant species, and it had almost completely replaced the $CO_2^-(H_2O)_n$ after 10 s (Figure 3c). The ADO efficiency of the core exchange can be roughly estimated to be 50%, assuming that the reverse reaction does not take place to any significant extent. This is significantly lower than the efficiency of the recombination reaction of O_2 with the solvated electron, indicating that the formation of the superoxide radical anion is not promoted by the presence of CO_2 in our experiment. Using similar arguments as above, the number of water molecules lost in the core exchange reaction is estimated to 3–4, so that the reaction can be summarized as in Equation (3).

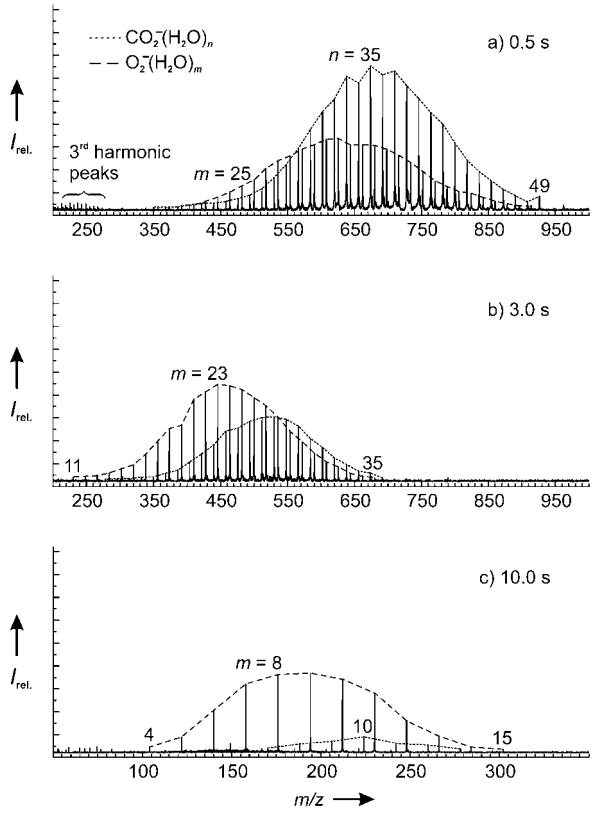

Figure 3. Mass spectra of the reaction of $(H_2O)_n^-$ with a roughly 2:1 mixture of CO_2 and O_2. a) After 0.5 s, $(H_2O)_n^-$ are completely converted to $CO_2^-(H_2O)_m$ and $O_2^-(H_2O)_m$, also in a ratio of roughly 2:1, despite the lower efficiency of the reaction of O_2 with $(H_2O)_n^-$. This indicates that core exchange has already occurred and that most $O_2^-(H_2O)_m$ originates from reactions with $CO_2^-(H_2O)_m$. b) After 3 s, the $O_2^-(H_2O)_m$ already dominate over the $CO_2^-(H_2O)_m$ to a level of ≈2:1. Again, black-body radiation and collision-induced dissociation lead to a gradual shrinking of the clusters. c) After 10 s, this process is almost complete, and $O_2^-(H_2O)_m$ are by far the dominant species in the mass spectrum.

$$CO_2^-(H_2O)_n^- + O_2 \rightarrow O_2^-(H_2O)_{n-x} + CO_2 + x\,H_2O,\ x \approx 3-4 \quad (3)$$

Quantum-chemical computations of hydrated CO_2^- and O_2^- anions: In order to obtain some additional insights into the structures and energetics of these ions, and to facilitate the interpretation of our observations, we carried out a series of computations on the stabilities, internal structures, and other properties of the $CO_2^-(H_2O)_n$ and $O_2^-(H_2O)_n$ species. The calculations were performed by using the commercial Gaussian 98 program package,[37] employing the hybrid, three-parameter density functional B3LYP method, as described by Becke,[38] with the Lee–Yang–Parr correlation functional,[39] as implemented in the Gaussian package. After pre-optimization with a smaller basis set, the full 6-311++G(3df,3pd) triple-zeta basis set, treating all electrons explicitly and employing one diffuse and four polarization functions on each atom, was used for geometry optimizations and frequency calculations. The basis set superposition error employing this large basis set is negligible, amounting to only about 5% of the total hydration energy estimated for the neutral clusters using the counterpoise method.

To obtain the structures, binding energies, as well as electron affinities, we carried out calculations on the H_2O fragment as well as on the $CO_2(H_2O)_n$, $CO_2^-(H_2O)_n$, $O_2(H_2O)_n$, and $O_2^-(H_2O)_n$ clusters, for $n = 0$–5. To verify that the optimized structures were true local minima, the vibrational frequencies were also computed for these species. Many of the clusters can exist in several "isomeric" forms, and in cases of doubt, computations with several different starting geometries were carried out. The structures shown in Figure 4 and Figure 5 are the optimized geometries with the lowest energy for $CO_2^-(H_2O)_n$ and $O_2^-(H_2O)_n$, respectively, with $n = 0$–5. The dissociation energies and electron affinities of the hydrated clusters, and the thermochemistry of the ionic core exchange reaction, are summarized in Table 1 and Table 2, respectively.

As already noted, carbon dioxide is a very stable molecule due to its closed-shell structure with 16 valence electrons and a completely filled highest occupied bonding π_g orbital. This, according to Walsh's rules, strongly favors a linear configuration and gives the molecule considerable rigidity and a rather high bending vibrational frequency, $\nu_2 = 668\ cm^{-1}$. Consistent with experiment, the computations predict that it requires considerable energy to place an additional electron into the next higher, empty "LUMO". This orbital is of π_u symmetry and, according to Walsh's rules, strongly favors a bent configuration. The resulting bent CO_2^- ion (Figure 4a) has a valence angle (138.2°) similar to that of the isoelectronic NO_2 (134.5°), both predicted by calculation at the B3LYP/6-311++G(3df,3pd) level of theory, but is quite unstable with respect to electron detachment. Our computation predicts the formation of the anion to be endothermic by 32.8 kJ mol^{-1}.

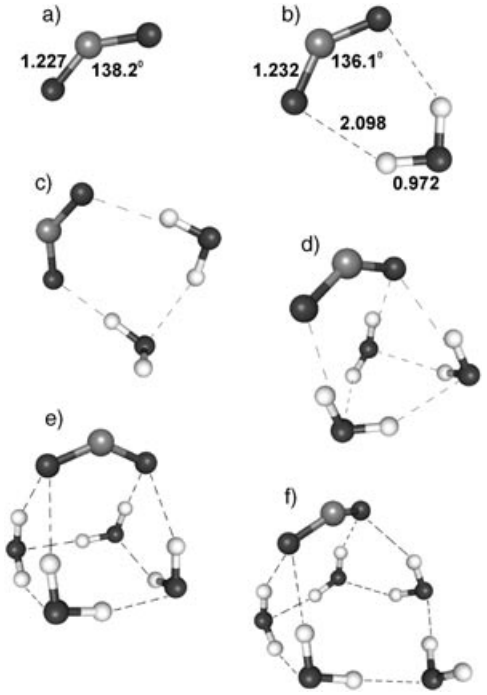

Figure 4. Optimized geometries of the most stable isomer of $CO_2^-(H_2O)_n$, $n = 1$–5 (bond distances in Å and bond angles in degrees). The geometries were evaluated by calculation at the B3LYP/6-311++G(3df,3pd) level of theory using the Gaussian 98 program. The CO_2^- is solvated on the cluster surface. The energies associated with water loss from the $CO_2^-(H_2O)_n$ clusters and the electron affinities of the corresponding neutral clusters are given in Table 1.

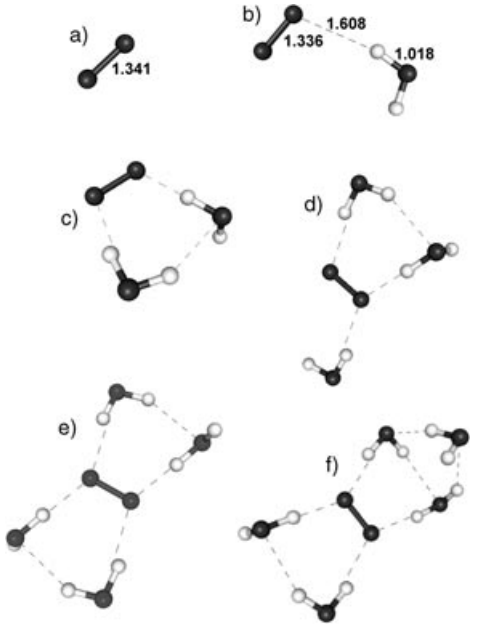

Figure 5. Optimized geometries of the most stable isomer of $O_2^-(H_2O)_n$, $n = 1$–5 (bond distances in Å and bond angles in degrees). The geometries were evaluated by calculation at the B3LYP/6-311++G(3df,3pd) level of theory using the Gaussian 98 program. The O_2^- is internally solvated. The energies associated with water loss from the $O_2^-(H_2O)_n$ clusters and the electron affinities of the corresponding neutral clusters are given in Table 1.

The situation is, however, quite different in aqueous solution. Even in the presence of a single H_2O molecule, the $CO_2\cdots H_2O$ complex has a positive electron affinity. The complex of neutral CO_2 with water, OCO···HOH, is only tenuously bound by a very weak hydrogen bond to one of the oxygen atoms of the CO_2. The binding energy is predicted to be less than 6 kJ mol^{-1}, and similarly weak binding energies are also predicted in the larger $CO_2\cdots(H_2O)_n$ clusters. In the presence of the extra electron, however, the linear, nonpolar carbon dioxide is converted into a bent, polar CO_2^- anion, which can form two strong hydrogen bonds to the two protons of the water molecule, forming a cyclic planar $CO_2^-\cdots H_2O$ species with C_{2v} symmetry (Figure 4b). The binding energy of the cyclic complex, computed to be 54.1 kJ mol^{-1}, more than offsets the endothermic nature of the free anion, so that the $CO_2\cdots H_2O$ complex has an electron affinity of 15.9 kJ mol^{-1}.

The larger neutral complexes are found to be essentially undistorted $(H_2O)_n$ clusters, that is, the $n = 2$ dimer and the cyclic $n = 3$, 4, and 5 polymers, with the CO_2 hydrogen-bonded to one of the free, dangling OH groups. Again, in

Table 1. Energies (in kJ mol^{-1}) of H_2O dissociation together with electron affinities (in kJ mol^{-1}) of $CO_2^-(H_2O)_n$ and $O_2^-(H_2O)_n$ including zero-point corrected (ZPC) energies, thermal enthalpies (ΔH), and thermal free energies (ΔG) under ambient conditions. All the energies were evaluated based on the optimized geometries for the most stable isomer at each cluster size n using the Gaussian 98 program at the B3LYP/6–311++G(3df,3pd) level of theory. The numbers in parentheses are experimental values.[a]

	$CO_2^-(H_2O)_n$					
n	Dissociation energy (D_o) $CO_2^-(H_2O)_n \rightarrow CO_2^-(H_2O)_{n-1} + H_2O$			Electron affinity $CO_2^-(H_2O)_n \rightarrow CO_2(H_2O)_n + e^-$		
	$\Delta E_{+\Delta ZPC}$	$\Delta H_{298\,K,1\,atm.}$	$\Delta G_{298\,K,1\,atm.}$	$\Delta E_{+\Delta ZPC}$	$\Delta H_{298\,K,1\,atm.}$	$\Delta G_{298\,K,1\,atm.}$
0				−32.8	−33.7	−26.0
1	54.1	56.9	22.1	15.9	19.2	1.3
2	45.2	48.0	12.7	45.2	47.4	43.9
3	40.1	44.3	0.2	63.7	66.7	48.0
4	41.4	44.4	5.3	64.3	66.1	56.3
5	31.2	34.3	−5.7	67.7	70.5	53.5
	$O_2^-(H_2O)_n$					
n	Dissociation energy (D_o) $O_2^-(H_2O)_n \rightarrow O_2^-(H_2O)_{n-1} + H_2O$			Electron affinity $O_2^-(H_2O)_n \rightarrow O_2(H_2O)_n + e^-$		
	$\Delta E_{+\Delta ZPC}$	$\Delta H_{298\,K,1\,atm.}$	$\Delta G_{298\,K,1\,atm.}$	$\Delta E_{+\Delta ZPC}$	$\Delta H_{298\,K,1\,atm.}$	$\Delta G_{298\,K,1\,atm.}$
0				50.1	50.1 (43.5)	49.6
1	82.3	86.0 (77.0)	55.9 (52.3)	113.4	138.5	119.9
2	62.7	66.3 (72.0)	27.2 (35)	184.5	191.8	163.0
3	53.0	54.4 (64.4)	21.6 (22)	208.7	212.0	195.0
4	45.8	48.8	9.8 (14)	216.0	218.1	202.7
5	35.0	38.5	−0.5	223.6	227.0	209.0

[a] NIST Chemistry WebBook, NIST Standard Reference Database Number 69, March 2003 (Eds.: P. J. Linstrom, W. G. Mallard) (http://webbook.nist.gov/chemistry/)

Table 2. Energies (in kJ mol^{-1}) of ionic core exchange of $CO_2^-(H_2O)_n$ and $O_2^-(H_2O)_n$ including zero-point corrected (ZPC) energies, thermal enthalpies (ΔH), and thermal free energies (ΔG) under ambient conditions. All of the energies were evaluated based on the optimized geometries for the most stable isomer at each cluster size n using the Gaussian 98 program at the B3LYP/6–311++G(3df,3pd) level of theory.

n	Ionic core exchange $CO_2^-(H_2O)_n + O_2 \rightarrow O_2^-(H_2O)_n + CO_2$		
	$\Delta E_{+\Delta ZPC}$	$\Delta H_{298\ K,1\ atm.}$	$\Delta G_{298\ K,1\ atm.}$
0	−82.9	−83.8	−75.6
1	−111.0	−112.8	−109.5
2	−128.5	−131.1	−124.0
3	−141.4	−141.2	−145.3
4	−145.8	−145.5	−149.9
5	−149.6	−149.7	−155.0

each case, the binding energy is very weak (less than 10 kJ mol^{-1}), and the potential surface is extremely flat. The anionic species are much more strongly bound. The $n = 2$ anion in Figure 4c is a distorted water dimer, in which each of the water molecules forms a hydrogen bond to one of the oxygen atoms of the CO_2^- ion. Similarly, the $n = 3$ and 4 species in Figure 4d and Figure 4e can be viewed as the cyclic water trimer and tetramer, respectively. In these cases, however, the water $(H_2O)_n$ species are strongly distorted compared with the free clusters. Unlike in the free $(H_2O)_3$ or $(H_2O)_4$, all of the "dangling" OH bonds are facing in the same direction, out of the plane defined by the water oxygen atoms, so that they can form hydrogen bonds to the negatively charged oxygen atoms of the CO_2^- anion. The $n = 5$ anion is again a cyclic water pentamer, but in this case, due to steric reasons, only four water molecules of the water pentamer are directly bound to the CO_2^- anion. The anions with $n > 1$ are stable with respect to electron detachment, with the solvation energies and the electron affinities increasing with n, as seen in Table 1.

The major differences in the energetics of the solvated molecular oxygen clusters are, as already mentioned, due to the fact that in contrast to carbon dioxide, in O_2 the antibonding $2p_{xy}\ \pi_g^*$ orbital is only partially occupied with two electrons, and can easily accommodate a third one, which results in the appreciable electron affinity of molecular dioxygen. The value that we computed, $E_A = 50.1$ kJ mol^{-1}, is in reasonable agreement with the experimental value of 43.5 kJ mol^{-1}.

The neutral complexes of O_2 with water are even more tenuously bound than those of CO_2, with computed binding energies being less than 1 kJ mol^{-1} for $n = 1$–5. In the $n = 1$ species, $O_2\cdots H_2O$, the oxygen molecule is hydrogen bonded with the O_2 being inclined at an angle of about 126.8° with respect to the nearly linear (174.1°) and rather long (2.454 Å) OH···O hydrogen bond. The structures of the larger, $n = 2$–5 $O_2(H_2O)_n$ species are quite similar to the corresponding neutral carbon dioxide complexes, consisting of essentially undistorted neutral $(H_2O)_n$ clusters with, in this case, the O_2 molecule being hydrogen-bonded to one of the dangling OH bonds.

The anionic $O_2^-\cdots H_2O$ is, unlike the corresponding complex of CO_2^-, not cyclic, but has planar C_s symmetry, with the O_2^- asymmetrically bound to one of the water protons (Figure 5b). The H···O bond in $O_2^-\cdots H_2O$ is much shorter (1.608 Å) than that in the neutral complex, with the O–O–H angle being 98.0°. The lowest-energy structures of the larger $O_2^-(H_2O)_n$ complexes, $n = 2$–4, are in agreement with recent ab initio studies.[23,24] Each water molecule hydrogen bonds to one of the four lobes of the in-plane $2p_{xy}\ \pi_g^*$ orbital of O_2^-. The complete first hydration shell contains four water molecules, $O_2^-(H_2O)_4$, which can be viewed as two water dimers interacting with the O_2^- (Figure 5e). As suggested by a recent photo-fragmentation experiment, $O_2^-(H_2O)_5$ was found to have a more complicated water network than in the case of $O_2^-(H_2O)_4$.[23,24] Indeed, the most stable structure of $O_2^-(H_2O)_5$ obtained (Figure 5f) contains a water dimer and a water trimer interacting separately with the ionic core O_2^-, so that the IR vibration pattern of $O_2^-(H_2O)_5$ is more complicated than that of $O_2^-(H_2O)_4$ (see the Supporting Information).

Hydration appreciably increases the electron affinities due to the formation of strong hydrogen bonds between the water ligands and the oxygen anion. As can be seen in Table 1, even for the $n = 1$ complex, $O_2\cdots H_2O$, the electron affinity is computed to be 113.4 kJ mol^{-1}, and it increases considerably further to more than 200 kJ mol^{-1} for the $n = 3$ species. On the other hand, the dissociation energies for the loss of water ligands from $O_2^-\cdots(H_2O)_n$ decrease in the same order as those in the case of $CO_2^-\cdots(H_2O)_n$, from 82.3 kJ mol^{-1} for the $n = 1$ complex to less than 40 kJ mol^{-1} for $n = 5$. In any event, for all the hydrated O_2^- clusters, the energies needed for electron detachment clearly considerably exceed those needed for the loss of a ligand.

Mechanism of the reactions of $(H_2O)_n^-$ clusters with O_2 and CO_2: With the results of the quantum-chemical computations, and with a better knowledge and understanding of the structures and bonding of the $O_2^-(H_2O)_n$ and $CO_2^-(H_2O)_n$ species, one can now consider in more detail the mechanism of the reactions observed here. There is a striking difference between the efficient reactions of the carbon dioxide and dioxygen molecules with the solvated $(H_2O)_n^-$ clusters, when compared with other similarly nonpolar molecules, such as, N_2[31] or ethylene, C_2H_4, or even the somewhat polar CO, which do not to react at all.

The key property here is their electron affinities, or, to be more precise, their abilities to exothermically bind an electron, thereby forming very stable anionic hydrates. Unlike the closed-shell N_2 and CO species with completely filled bonding $2p_{xy}\ \pi_u$ orbitals, the highest, doubly occupied antibonding $2p_{xy}\ \pi_g^*$ orbitals of O_2 can accommodate a third electron, resulting in the appreciable electron affinity of molecular oxygen of 50.1 kJ mol^{-1}. Upon collision with $(H_2O)_n^-$, the O_2^- that is immediately formed is further strongly stabilized by the water ligands. In the case of CO_2, the two highest π_g molecular orbitals of which are fully occupied by four electrons, the electron affinity is, in contrast to that of O_2, negative (−32.8 kJ mol^{-1}). CO_2 has, however, an empty, low-lying π_u orbital that can accept an extra electron, resulting in a bent, polar CO_2^- ion, isoelectronic with NO_2. The naked anion is unstable with respect to auto-detachment, but it can be stabilized by hydration. A cyclic

$CO_2^-\cdots H_2O$ anion complex is formed even in the presence of a single water ligand, since the binding energies of its two strong hydrogen bonds more than compensate for the endothermic nature of the free CO_2^-, and the anion is further stabilized by additional water ligands.

Clearly, the key difference here is the existence of low-lying unfilled or partially filled orbitals in the case of CO_2 and O_2, and their absence in the other species such as N_2, CO, or ethylene, C_2H_4, which do not react with hydrated electron clusters. These molecules without low-lying, unoccupied orbitals cannot bind an extra electron. Their presence is evidenced only by their slight contribution to the rates of cluster fragmentation. While the exact location of the negative charge in the $(H_2O)_n^-$ solvated electron clusters is still controversial, it is undoubtedly fairly diffuse and probably localized at the cluster surface. During the collision of the gaseous reactant molecule with the solvated electron, a charge transfer takes place, with the O_2^- or CO_2^- anion formed being immediately stabilized by strong hydrogen bonds to the cluster surface. The fact that the process occurs efficiently not only with molecular oxygen, but also with CO_2, the electron affinity of which is negative, suggests that the charge-transfer and the anion stabilization by hydrogen-bond formation have to be considered as concurrent rather than consecutive reaction steps.

Since the aforementioned mechanistic interpretation of the process requires the availability of a free electron, one can also easily understand the fact that one and only one molecule of CO_2 or O_2 can be taken up by the cluster anion. Once the electron is intimately bound to form the anion, and stabilized by the water ligands, it is no longer available to enable a further molecule to enter the cluster. By the same argument, one can also explain the lack of reactivity of carbon dioxide with a large number of other hydrated ions, whether positively or negatively charged, in which a free electron is not available.

In the light of the results of the computations, one can also immediately understand the different number of water molecules lost in reactions (1) and (2). As can be seen in Table 1, the dissociation energies of the hydrated O_2^- and CO_2^- clusters are fairly similar. The electron affinities of $O_2\cdots(H_2O)_n$ are, however, some 150 kJ mol^{-1} higher than those of $CO_2\cdots(H_2O)_n$, which means that much more energy will be released during the reaction of O_2 with the hydrated electron, and this is responsible for the evaporation of several more water ligands. In addition, the thermodynamics of the reactions can also explain some features of the cluster fragmentation. As can be seen in Table 1, for both $CO_2^-(H_2O)_n$ and $O_2^-(H_2O)_n$ the electron affinities increase, but the energies required for the loss of water ligand decrease, with increasing n. For $CO_2^-(H_2O)_n$ with $n>2$, the energies required to evaporate a water molecule are smaller than those needed to detach an electron, and this difference is even more pronounced if entropic effects are considered, as shown by the free energies in Table 1. Accordingly, for the larger clusters, fragmentation is observed, with no evidence of ions being lost in the FT-ICR experiments. For the small $CO_2^-(H_2O)_n$ complexes ($n\leq 2$) the situation is reversed, with the energies favoring electron detachment. These computational results are in excellent agreement with our experimental observations, with the small anions gradually disappearing from the cell, and with $CO_2^-\cdots H_2O$ ($n = 1$) not being detected at all. Ultimately, after a reaction time of about 40 s, all the ions have lost the electron and completely disappeared from the mass spectrum, the lower detection limit of which is $m/z = 14.5$ amu.

A considerably different situation prevails for the $O_2^-(H_2O)_n$ anions, as can also be seen in Table 1. Here, even for the $O_2^-H_2O$ anion ($n = 1$) the computed ionization energy of 113.4 kJ mol^{-1} considerably exceeds the dissociation energy of 82.3 kJ mol^{-1}, and the ionization energies for the larger species are in excess of 200 kJ mol^{-1}. As already noted, the dissociation energies decrease with n, and at least for $n = 1$ and 2 they are larger than those of the hydrated CO_2^- anion by some 15 kJ mol^{-1}. Accordingly, the fragmentation slows down considerably for the smallest ions, and near the end of the fragmentation process, $O_2^-(H_2O)_3$ is only very slowly converted to $O_2^-(H_2O)_2$, with no $O_2^-(H_2O)$ being detected. Electron detachment, if it occurs at all, must be exceedingly slow, even on the time scale of our experiment. Accordingly, in experiments with molecular O_2, the $O_2^-(H_2O)_n$ $n = 2$ and 3 clusters effectively remain even after the longest times studied. In some experiments involving CO_2, in which small amounts of O_2 impurities were present, these $n = 2$ and 3 oxygen-containing clusters remained even after all the $CO_2^-(H_2O)_n$ anions had undergone electron detachment.

The computed relative stabilities of $CO_2^-(H_2O)_n$ and $O_2^-(H_2O)_n$ were also confirmed by mixed experiments, in which both CO_2 and O_2 were introduced into the FT-ICR trap. The ionic core of $CO_2^-(H_2O)_n$ slowly exchanges from CO_2^- to O_2^-, which is also indicative of the greater exothermicity of the formation of $O_2^-(H_2O)_n$ as compared with the formation of $CO_2^-(H_2O)_n$. Table 2 shows the reaction energy of the ionic core exchange process. For the naked anions, the reaction energy of the ionic core exchange is the difference in the electron affinities of CO_2 and O_2, which is already -82.9 kJ mol^{-1}. The ionic core exchange becomes more exothermic as the cluster size increases. The reaction is exothermic by up to 150 kJ mol^{-1} for a cluster size of $n = 5$, which suggests that the energy released in the exchange of the anionic core is also sufficient for the observed loss of three to four water molecules.

Based on the present results, it is of course not possible to ascertain whether the molecular anion formed remains on the surface of the water cluster, or migrates inside it to become internally solvated. It seems that the solvation structure depends on the electronic structure and the geometry of the anionic core. For example, for clusters with up to five water molecules, the bent CO_2^- prefers solvation at the surface, while O_2^- favors internal solvation because of its symmetrical electronic structure.

The observations reported here are also of some relevance to our earlier studies on hydrated Mg^+ cations.[40,41] In order to rationalize some reactions of these species, we and others have argued that when placed into an aqueous cluster, a second ionization may take place, so that the $Mg^+(H_2O)_n$ species actually contain an Mg^{2+} ion and an elec-

tron.[40–45] The fact that these clusters were also found to be unreactive towards CO_2, and that no carbonate formation could be detected, suggests that if such a second ionization does take place, the electron is not really free and available to enable the CO_2 molecule to enter the cluster.

Conclusion

We have investigated the gas-phase reactions of CO_2 and O_2 molecules with solvated electron clusters $(H_2O)_n^-$. The reactions proceed by the formation of CO_2^- or O_2^- molecular anions and their concurrent hydration. Since a single electron is present, one and only one molecule can be taken up by the cluster. These anionic clusters then gradually fragment under the influence of black-body radiation and collisions with the reaction gas. In the case of $CO_2^-(H_2O)_n$, the fragmentation proceeds down to the $n = 2$ cluster, which eventually undergoes detachment of the electron and vanishes from the ICR trap. For the more stable $O_2^-(H_2O)_n$, fragmentation also results in the $n = 2$ species, which is, however, a stable final product that, under the conditions of our experiments, neither further fragments nor undergoes detachment of the electron. The experimental study has been accompanied by a series of quantum-chemical calculations on the structures, stabilities, and energetics of the species studied, which have aided the interpretation of our observations. For clusters with size up to $n = 5$, the CO_2^- resides on the cluster surface, while O_2^- is internally solvated.

Experimental Section

The experimental methods used here were analogous to those used in our previous studies, which were described in detail in the associated reports.[3,33] The hydrated electron clusters, $(H_2O)_n^-$, were produced in a laser vaporization cluster source[46–48] developed in our laboratory.[49,50] In the source, a pulsed Nd:YAG laser beam impinges upon a metal target in the presence of a high pressure of an inert carrier gas, usually helium (10 bar). The flow of the gas, containing water with its room temperature vapor pressure as partial pressure, is controlled by a piezoelectric valve, the opening of which is synchronized with the laser pulse. Depending on the exact conditions, the source can produce a relatively wide distribution of the solvated electron clusters, where the number of ligands, n, can range from 15 to nearly 100. A rapid fragmentation of the aqueous clusters due to absorption of the ambient black-body infrared radiation limits the upper end of the distribution, while the formation of smaller clusters below about $n = 20$ becomes increasingly inefficient due to their low electron affinity and rapid electron detachment.[33]

The ion clusters that are formed in the source and during the adiabatic expansion into high vacuum are guided along the magnetic field axis through several stages of differential pumping into the ICR cell. This is located inside the bore of the 4.7 T superconducting magnet of our Bruker/Spectrospin CMS47X FT-ICR mass spectrometer, which is equipped with an APEX III data station. At the start of each measurement, clusters produced in about twenty vaporization pulses are accumulated in the ICR cell.

To study chemical reactions, the reactant gases, in the present case mainly carbon dioxide or oxygen, are admitted into the instrument via a leak valve, to raise the pressure of the high vacuum section from the background value in the low 10^{-11} mbar range to a stable value usually in the range of about $2–5\times10^{-9}$ mbar. To obtain information about the cluster formation, their reactions, and the kinetics of their fragmentation, mass spectra are acquired at a nominal time of $t = 0$ s, that is, immediately after completion of the accumulation, and then after allowing the reaction to proceed for various delays typically ranging up to 50 s.

The simultaneous presence of hydrated metal anions in our previous study[33] did not interfere with the experiment, and in fact provided a useful means of proving that the electrons were indeed being detached from the clusters. In the work described here, however, which was aimed at exploring chemical reactions of the electrons, the formation of $M^-(H_2O)_n$ could be avoided by employing targets made of metals with closed-shell structures and zero electron affinity. As shown previously,[3] the use of zinc results in exclusive formation of the desired $(H_2O)_n^-$ clusters.

Acknowledgements

Financial support from the Deutsche Forschungsgemeinschaft, the European Union through the Research Training Network "Reactive Intermediates Relevant in Atmopheric Chemistry and Combustion", and the Fonds der Chemischen Industrie is gratefully acknowledged.

[1] G. V. Buxton, C. L. Greenstock, W. P. Helman, A. B. Ross, *J. Phys. Chem. Ref. Data* **1988**, *17*, 513–886.
[2] R. A. Marcus, *Rev. Mod. Phys.* **1993**, *65*, 599–610.
[3] O. P. Balaj, I. Balteanu, B. S. Fox-Beyer, M. K. Beyer, V. E. Bondybey, *Angew. Chem.* **2003**, *115*, 5675–5677; *Angew. Chem. Int. Ed.* **2003**, *42*, 5516–5518.
[4] M. E. Jacox, D. E. Milligan, *Chem. Phys. Lett.* **1974**, *28*, 163–168.
[5] Z. H. Kafafi, R. H. Hauge, W. E. Billups, J. L. Margrave, *Inorg. Chem.* **1984**, *23*, 177–183.
[6] M. E. Jacox, W. E. Thompson, *J. Chem. Phys.* **1989**, *91*, 1410–1416.
[7] W. E. Thompson, M. E. Jacox, *J. Chem. Phys.* **1999**, *111*, 4487–4496.
[8] M. F. Zhou, L. Andrews, *J. Chem. Phys.* **1999**, *110*, 6820–6826.
[9] M. F. Zhou, L. Andrews, *J. Chem. Phys.* **1999**, *110*, 2414–2422.
[10] R. N. Compton, P. W. Reinhardt, C. D. Cooper, *J. Chem. Phys.* **1975**, *63*, 3821–3827.
[11] M. J. W. Boness, G. J. Schulz, *Phys. Rev. A* **1974**, *9*, 1969–1979.
[12] Y. Yoshioka, K. D. Jordan, *Chem. Phys. Lett.* **1981**, *84*, 370–374.
[13] K. D. Jordan, *J. Phys. Chem.* **1984**, *88*, 2459–2465.
[14] C. E. Klots, R. N. Compton, *J. Chem. Phys.* **1977**, *67*, 1779–1780.
[15] C. E. Klots, R. N. Compton, *J. Chem. Phys.* **1978**, *69*, 1636–1643.
[16] A. R. Rossi, K. D. Jordan, *J. Chem. Phys.* **1979**, *70*, 4422–4424.
[17] C. E. Klots, *J. Chem. Phys.* **1979**, *71*, 4172–4172.
[18] T. Tsukuda, M. Saeki, R. Kimura, T. Nagata, *J. Chem. Phys.* **1999**, *110*, 7846–7857.
[19] M. Saeki, T. Tsukuda, S. Iwata, T. Nagata, *J. Chem. Phys.* **1999**, *111*, 6333–6344.
[20] E. Surber, S. P. Ananthavel, A. Sanov, *J. Chem. Phys.* **2002**, *116*, 1920–1929.
[21] B. H. J. Bielski, D. E. Cabelli, R. L. Arudi, A. B. Ross, *J. Phys. Chem. Ref. Data* **1985**, *14*, 1041–1100.
[22] W. H. Koppenol, J. D. Rush, *J. Phys. Chem.* **1987**, *91*, 4429–4430.
[23] J. M. Weber, J. A. Kelley, S. B. Nielsen, P. Ayotte, M. A. Johnson, *Science* **2000**, *287*, 2461–2463.
[24] J. M. Weber, J. A. Kelley, W. H. Robertson, M. A. Johnson, *J. Chem. Phys.* **2001**, *114*, 2698–2706.
[25] H. Haberland, C. Ludewigt, H. G. Schindler, D. R. Worsnop, *J. Chem. Phys.* **1984**, *81*, 3742–3744.
[26] H. Haberland, H. Langosch, H. G. Schindler, D. R. Worsnop, *J. Phys. Chem.* **1984**, *88*, 3903–3904.
[27] H. Haberland, H. G. Schindler, D. R. Worsnop, *Ber. Bunsen-Ges.* **1984**, *88*, 270–272.
[28] L. A. Posey, M. A. Johnson, *J. Chem. Phys.* **1988**, *89*, 4807–4814.
[29] J. V. Coe, G. H. Lee, J. G. Eaton, S. T. Arnold, H. W. Sarkas, K. H. Bowen, C. Ludewigt, H. Haberland, D. R. Worsnop, *J. Chem. Phys.* **1990**, *92*, 3980–3982.
[30] G. H. Lee, S. T. Arnold, J. G. Eaton, H. W. Sarkas, K. H. Bowen, C. Ludewigt, H. Haberland, *Z. Phys. D* **1991**, *20*, 9–12.
[31] L. A. Posey, M. J. Deluca, P. J. Campagnola, M. A. Johnson, *J. Phys. Chem.* **1989**, *93*, 1178–1181.

[32] S. T. Arnold, R. A. Morris, A. A. Viggiano, M. A. Johnson, *J. Phys. Chem.* **1996**, *100*, 2900–2906.
[33] M. K. Beyer, B. S. Fox, B. M. Reinhard, V. E. Bondybey, *J. Chem. Phys.* **2001**, *115*, 9288–9297.
[34] T. Su, M. T. Bowers, *J. Chem. Phys.* **1973**, *58*, 3027–3037.
[35] L. Bass, T. Su, M. T. Bowers, *Int. J. Mass Spectrom. Ion Processes* **1978**, *28*, 389–399.
[36] L. Bass, T. Su, W. J. Chesnavich, M. T. Bowers, *Chem. Phys. Lett.* **1975**, *34*, 119–122.
[37] M. J. Frisch, G. W. Trucks, H. B. Schlegel, G. E. Scuseria, M. A. Robb, J. R. Cheeseman, V. G. Zakrzewski, J. A. Montgomery, Jr., R. E. Stratmann, J. C. Burant, S. Dapprich, J. M. Millam, A. D. Daniels, K. N. Kudin, M. C. Strain, O. Farkas, J. Tomasi, V. Barone, M. Cossi, R. Cammi, B. Mennucci, C. Pomelli, C. Adamo, S. Clifford, J. Ochterski, G. A. Petersson, P. Y. Ayala, Q. Cui, K. Morokuma, D. K. Malick, A. D. Rabuck, K. Raghavachari, J. B. Foresman, J. Cioslowski, J. V. Ortiz, B. B. Stefanov, G. Liu, A. Liashenko, P. Piskorz, I. Komaromi, R. Gomperts, R. L. Martin, D. J. Fox, T. Keith, M. A. Al-Laham, C. Y. Peng, A. Nanayakkara, C. Gonzalez, M. Challacombe, P. M. W. Gill, B. G. Johnson, W. Chen, M. W. Wong, J. L. Andres, M. Head-Gordon, E. S. Replogle, J. A. Pople, Gaussian 98, Revision A.9, Gaussian, Inc., Pittsburgh, PA, **1998**.
[38] A. D. Becke, *J. Chem. Phys.* **1993**, *98*, 5648–5652.
[39] C. T. Lee, W. T. Yang, R. G. Parr, *Phys. Rev. B* **1988**, *37*, 785–789.
[40] C. Berg, M. Beyer, U. Achatz, S. Joos, G. Niedner-Schatteburg, V. E. Bondybey, *Chem. Phys.* **1998**, *239*, 379–392.
[41] C. Berg, U. Achatz, M. Beyer, S. Joos, G. Albert, T. Schindler, G. Niedner-Schatteburg, V. E. Bondybey, *Int. J. Mass Spectrom.* **1997**, *167*, 723–734.
[42] K. Fuke, K. Hashimoto, S. Iwata, in *Adv. Chem. Phys.*, *Vol. 110*, **1999**, pp. 431–523.
[43] B. M. Reinhard, G. Niedner-Schatteburg, *J. Chem. Phys.* **2003**, *118*, 3571–3582.
[44] C. K. Siu, Z. F. Liu, *Chem. Eur. J.* **2002**, *8*, 3177–3186.
[45] B. M. Reinhard, G. Niedner-Schatteburg, *Phys. Chem. Chem. Phys.* **2002**, *4*, 1471–1477.
[46] V. E. Bondybey, J. H. English, *J. Chem. Phys.* **1981**, *74*, 6978–6979.
[47] T. G. Dietz, M. A. Duncan, D. E. Powers, R. E. Smalley, *J. Chem. Phys.* **1981**, *74*, 6511–6512.
[48] S. Maruyama, L. R. Anderson, R. E. Smalley, *Rev. Sci. Instrum.* **1990**, *61*, 3686–3693.
[49] C. Berg, T. Schindler, G. Niedner-Schatteburg, V. E. Bondybey, *J. Chem. Phys.* **1995**, *102*, 4870–4884.
[50] M. Beyer, C. Berg, H. W. Görlitzer, T. Schindler, U. Achatz, G. Albert, G. Niedner-Schatteburg, V. E. Bondybey, *J. Am. Chem. Soc.* **1996**, *118*, 7386–7389.

Received: April 28, 2004
Published online: August 17, 2004

